JOURNAL OF THE HYDRAULICS DIVISION

Coupled Dynamic Streamflow-Temperature Models

By David S. Bowles,[1] A. M. ASCE, Danny L. Fread,[2]
and William J. Grenney,[3] Members, ASCE

Introduction

Temperature is perhaps the single most important parameter in stream-water quality. Human activity generally raises natural stream-water temperatures due to impoundments, industrial uses, irrigation, and modifications of topographic features. As a result, higher temperatures reduce the solubility of dissolved oxygen, increase metabolism, respiration, and oxygen demand of aquatic life, intensify many types of toxicity, and promote "less desirable" fish species and aquatic organisms (8). Numerous mathematical models of the mechanisms of heat transfer in streams are now available. In contrast to most of the previous models, the stream temperature model described in this paper is dynamic and can be used in conjunction with a dynamic streamflow model. The Dynamic Stream Temperature Model (DSTEMP) may be used for prediction of stream temperatures over a diurnal cycle or over extended periods of time. The DSTEMP can be applied to small streams in which streambed heat exchange is important (5), or it can be applied to large river systems with first-order tributaries, thermal discharges, and meteorologic conditions that vary spatially over the river basin (4). Data requirements are realistic in terms of data types usually collected by the National Weather Service, National Atmospheric and Oceanic Administration (NOAA), and the United States Geological Survey (USGS). An unsteady flow model (6,7) was linked to the DSTEMP model, and the combined model (SNRT-DSTEMP) was applied to the Brazos-Little River System, Texas. A 12-hr computational time interval is used for the simulation of a flood of 23 days duration.

MODEL DESCRIPTION

Implicit Dynamic Routing Program (DNRT).—The DNRT is a streamflow routing model for computing transient stages and discharges at selected points along a river from a given stage or discharge hydrograph at the upstream boundary of a river reach in which a flood wave is propagating (7). The interaction of storage and dynamic effects between a river and its tributaries may be efficiently simulated using DNRT (6). The DNRT model is based on the complete one-dimensional unsteady flow equations, i.e.

$$\frac{\partial Q}{\partial x} + \frac{\partial A}{\partial t} - Q_l = 0 \quad \dots \dots \dots \dots \dots \dots \dots \dots \dots \dots \dots \dots (1)$$

$$\frac{\partial Q}{\partial t} + \frac{\partial (Q^2/A)}{\partial x} + gA\left(\frac{\partial H}{\partial x} + S_f\right) - Q_1 U_{1x} = 0 \quad \dots \dots \dots \dots \dots \dots (2)$$

in which $\quad S_f = 0.45 n^2 Q^2 A^{-2} R^{-4/3} \quad \dots \dots \dots \dots \dots \dots \dots \dots (3)$

and Q = streamflow rate, in cubic feet per second; A = cross-sectional area of stream, in square feet; Q_l = rate of surface lateral inflow per unit length of stream, in square feet per second; ∂t = computational time interval, in seconds; ∂x = computational space interval or subreach length, in feet (positive in the downstream direction); g = acceleration due to gravity, in feet per second^2; H = water surface elevation, in feet; S_f = friction slope, in feet per foot; U_{1x} = velocity of surface lateral inflow in direction of streamflow, in feet per second; n = Manning roughness coefficient, in feet$^{1/6}$; and R = hydraulic radius of stream cross section, in feet. The unsteady flow equations are solved by an implicit weighted four-point finite difference method. The resulting system of nonlinear algebraic equations are solved by the Newton-Raphson iterative method used in conjunction with an extrapolation technique and a special quad-diagonal Gaussian elimination procedure. The DNRT has been verified on several floods and hurricane surges in the Lower Mississippi River and the lower portion of the Ohio-Mississippi River system. The hydraulic and stream geometry data transferred to DSTEMP from DNRT include: Computational time intervals; subreach lengths; cross-sectional areas; top widths of flow; wetted perimeters; streamflow rates; stream stages; and surface lateral inflow rates.

DSTEMP Model Formulation.—The model for prediction of average and diurnal stream temperatures is formulated by performing a heat balance on a control volume in the stream. Two important assumptions are made: Complete and instantaneous mixing over each stream cross section; and negligible longitudinal dispersion. The validity of these assumptions should be reconsidered before applying the model to a new problem or to a new river.

Four types of heat flux are considered in the heat balance on the control volume (Fig. 1): (1) Nonadvective heat exchange across the stream surface; (2) nonadvective heat exchange across the streambed; (3) advection of heat associated with stream velocity; and (4) other advective heat fluxes by lateral inflow, tributary inflow, ground-water infiltration and seepage, rainfall and snowfall, and evaporation. A heat balance over the time interval, dt, for the

subreach control volume shown in Fig. 1 is obtained by equating the sum of the four types of heat flux to the net change in total heat contained in the

(a) Stream geometry

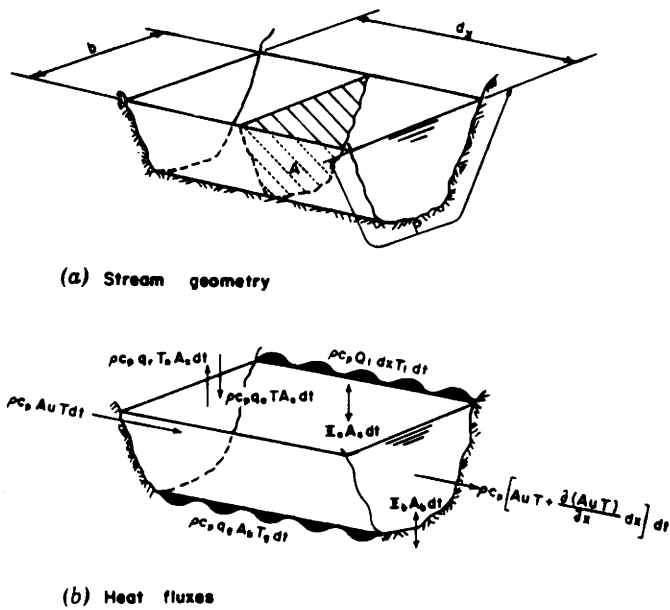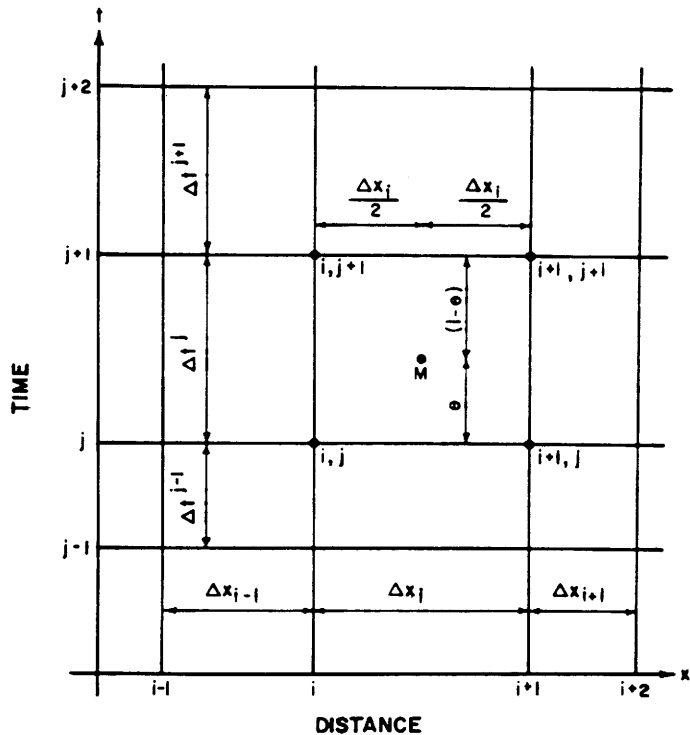(b) Heat fluxes

FIG. 1.—Subreach Control Volume

FIG. 2.—Network of Points on (x, t) Plane for Weighted Implicit Four-Point Finite Difference Method (1)

control volume. The sign convention adopted is positive for advection of mass into the stream. Heat exchange, such as radiation, which is not associated with mass transfer is treated as positive when the transfer of heat is into the stream.

When water leaves the stream by overbank spill, diversions, or seepage, the rates of surface (Q_l) or ground-water (q_g) lateral inflow are negative. In these cases, the temperature of water leaving the stream is the stream temperature, T. Therefore, advective terms associated with Q_l and q_g are each separated into two terms according to the signs of Q_l and q_g. If Q_l and q_g are positive (Q_l^+, q_g^+), then the temperatures, T_l and T_g, are used respectively. The variable, T_l, is the temperature of surface lateral inflow, in degrees Fahrenheit, and T_g is the ground-water temperature, in degrees Fahrenheit. When Q_l and q_g are negative (Q_l^-, q_g^-), then T is used instead of T_l and T_g.

Net surface and streambed exchange, Φ_s and Φ_b are each calculated from the summation of a number of component heat transfers, described as follows:

1. Heat balance—$\Phi_s = (\phi_s - \phi_{sr}) + (\phi_v - \phi_{vr}) + (\phi_a - \phi_{ar}) - \phi_b - \phi_e + \phi_c - \phi_{sn} - \phi_w$; $\Phi_b = \phi_{bs} + \phi_{bb} + \phi_{bc}$.

2. Solar radiation, ϕ_S, ϕ_{sr}: (1) $\phi_r = f(\phi, \alpha, \alpha_{sr}, \alpha_{ss}, D, R_g, R_t, d_p, S, C)$ (13), $\phi_{sr} = R_t \phi_s$; (2) by parabolic distribution of observed solar radiation between sunrise and sunset; or (3) by direct use of observed solar radiation.

3. Vegetative radiation, ϕ_v, ϕ_{vr}—$\phi_v = \sigma(T_a + 460)^4$ (10); $\phi_{vr} = R_l \phi_v$.

4. Atmospheric radiation, ϕ_a—$\phi_a = \beta\sigma(T_a + 460)^4$ (11); $\phi_{ar} = R_l \phi_v$.

5. Back radiation, ϕ_b—$\phi_b = 0.97\sigma(T_a + 460)^4$ (2).

6. Evaporation, ϕ_e—$\phi_e = 1.47\rho L_v Nu(e_s - e_a)$ (13).

7. Conduction, ϕ_c—$\phi_c = 0.217(T - T_a)/(e_s - e_a)P_a \phi_e$ (3).

8. Melting snow, ϕ_{sn}—$\phi_{sn} = q_{sn}\rho[L_f + c_{sn}(T - T_r)]$.

9. Surface layer renewal, ϕ_w—$\phi_w = 3.96 \times 10^4 k(U/h)^{0.33}(T_s - T)$ (9).

10. Streambed solar radiation, ϕ_{bs}—$\phi_{bs} = (1 - s)(1 - R_b)(\phi_s - \phi_{sr}) \exp(-\eta h)$.

11. Streambed back radiation, ϕ_{bb}—$\phi_{bb} = \epsilon\sigma(T_b + 460)^4$.

12. Streambed conduction, ϕ_{bc}—$\phi_{bc} = \alpha_1 + \alpha_2\phi_{bs} + \alpha_3 T_g + \alpha_4 T$ (5).

13. Other terms—Point loads $T' = (QT + Q_p T_p)/(Q + Q_p)$.

Some of these equations are nonlinear in T, and to simplify the numerical solution procedures, most stream temperature models employ a linear approximation for Φ_s and Φ_b. In DSTEMP, empirical linear approximations, piecewise-linear approximations, and least-squares linear approximations to nonlinear components of Φ_s and Φ_b are employed. Thus, Φ_s and Φ_b are expressed in the linear forms as

$$\Phi_s = C_1 + C_2 T = \sum_{i=1}^{n} (c_1^i + c_2^i T) \quad\dots\dots\dots\dots\dots (4)$$

$$\Phi_b = C_3 + C_4 T = \sum_{i=1}^{m} (c_3^i + c_4^i T) \quad\dots\dots\dots\dots\dots (5)$$

in which T = stream temperature, in degrees Fahrenheit; C_1, C_2, C_3, C_4, c_1^i, c_2^i, c_3^i, and c_4^i = coefficients; each of the n components of Φ_s are expressed in the linear form $c_1^i + c_2^i T$; and each of the m components of Φ_b are expressed in the linear form $c_3^i + c_4^i T$.

The final equation resulting from the preceding considerations is

$$\frac{\partial(AT)}{\partial t} + \frac{\partial(QT)}{\partial x} - \left[\frac{bC_1 + PC_3}{\rho c_p} + Q_l^+ T_l + q_g^+ PT_g + q_r bT_r \right]$$

$$- \left[\frac{bC_2 + PC_4}{\rho c_p} + Q_l^- + q_g^- P - q_e b \right] T = 0 \quad \dots \dots \dots \dots \dots \dots \quad (6)$$

in which ρ = density of water, in pounds per cubic foot; q_g = rate of ground-water lateral inflow per unit area of streambed (+ superscript indicates flow into stream, − superscript indicates flow out of stream), in cubic feet per second per square foot; T_g = ground-water temperature in degrees Fahrenheit; q_r = precipitation rate, in feet per second; T_r = wet-bulb temperature, in degrees Fahrenheit; b = top breadth of stream, in feet; c_p = specific heat of water at constant pressure, in British thermal units per pound per degree Fahrenheit; P = wetted perimeter of stream, in feet; Q_l = rate of surface lateral inflow (overland flow plus interflow per unit length of subreach, + superscript indicates flow into stream, − superscript indicates flow out of stream), in cubic feet per second per foot; q_e = evaporation rate, in feet per second; T = stream temperature, in degrees Fahrenheit; and T_l = temperature of surface lateral inflow, in degrees Fahrenheit.

Numerical Solution

Implicit Four-Point Finite Difference Scheme.—Explicit finite difference techniques applied to the solution of the unsteady flow equations are restricted by numerical stability considerations to very small computational time steps of the order of minutes or seconds. Therefore, the explicit method is very inefficient for stream simulations lasting several days or weeks. In contrast, implicit finite difference techniques have no restrictions on the size of the specified time interval, due to computational stability; however, accuracy constraints may limit its size. The implicit weighted four-point finite difference scheme utilized by Fread in DNRT allows for variable size space intervals Δx and time intervals Δt. Fig. 2 contains a four-point grid identified by the intersections of the vertical lines, x_i and x_{i+1}, with the horizontal lines, t^j and t^{j+1}. Finite differencing is carried out for a point M within the four-point grid. At the point, M, the value of a function, $K(M)$, is represented by

$$K(M) \simeq \theta \frac{K_i^{j+1} + K_{i+1}^{j+1}}{2} + (1 - \theta) \frac{K_i^j + K_{i+1}^j}{2} \quad \dots \dots \dots \dots \quad (7)$$

in which θ = a weighting factor determining the location of M between the two adjacent time lines t^j and t^{j+1}. Space and time partial derivatives of $K(M)$ are approximated by

$$\frac{\partial K(M)}{\partial x} \simeq \theta \frac{K_{i+1}^{j+1} - K_i^{j+1}}{\Delta x_i} + (1 - \theta) \frac{K_{i+1}^j - K_i^j}{\Delta x_i} \dots \dots \dots \dots \dots \quad (8)$$

$$\frac{\partial K(M)}{\partial t} \simeq \frac{K_i^{j+1} + K_{i+1}^{j+1} - K_i^j - K_{i+1}^j}{2\Delta t^j} \quad \dots \dots \dots \dots \dots \dots \quad (9)$$

The second writer (7) found that for slowly varying transients in large rivers, $\theta = 0.55$ minimizes the loss of accuracy associated with greater values while

$$\frac{\partial(AT)}{\partial t} + \frac{\partial(QT)}{\partial x} - \left[\frac{bC_1 + PC_3}{\rho c_p} + Q_l^+ T_l + q_g^+ PT_g + q_r bT_r\right]$$

$$- \left[\frac{bC_2 + PC_4}{\rho c_p} + Q_l^- + q_g^- P - q_e b\right] T = 0 \quad \dots \dots \dots \dots \dots \quad (6)$$

in which ρ = density of water, in pounds per cubic foot; q_g = rate of ground-water lateral inflow per unit area of streambed (+ superscript indicates flow into stream, − superscript indicates flow out of stream), in cubic feet per second per square foot; T_g = ground-water temperature in degrees Fahrenheit; q_r = precipitation rate, in feet per second; T_r = wet-bulb temperature, in degrees Fahrenheit; b = top breadth of stream, in feet; c_p = specific heat of water at constant pressure, in British thermal units per pound per degree Fahrenheit; P = wetted perimeter of stream, in feet; Q_l = rate of surface lateral inflow (overland flow plus interflow per unit length of subreach, + superscript indicates flow into stream, − superscript indicates flow out of stream), in cubic feet per second per foot; q_e = evaporation rate, in feet per second; T = stream temperature, in degrees Fahrenheit; and T_l = temperature of surface lateral inflow, in degrees Fahrenheit.

Numerical Solution

Implicit Four-Point Finite Difference Scheme.—Explicit finite difference techniques applied to the solution of the unsteady flow equations are restricted by numerical stability considerations to very small computational time steps of the order of minutes or seconds. Therefore, the explicit method is very inefficient for stream simulations lasting several days or weeks. In contrast, implicit finite difference techniques have no restrictions on the size of the specified time interval, due to computational stability; however, accuracy constraints may limit its size. The implicit weighted four-point finite difference scheme utilized by Fread in DNRT allows for variable size space intervals Δx and time intervals Δt. Fig. 2 contains a four-point grid identified by the intersections of the vertical lines, x_i and x_{i+1}, with the horizontal lines, t^j and t^{j+1}. Finite differencing is carried out for a point M within the four-point grid. At the point, M, the value of a function, $K(M)$, is represented by

$$K(M) \simeq \theta \frac{K_i^{j+1} + K_{i+1}^{j+1}}{2} + (1 - \theta) \frac{K_i^j + K_{i+1}^j}{2} \quad \dots \dots \dots \dots \dots \quad (7)$$

in which θ = a weighting factor determining the location of M between the two adjacent time lines t^j and t^{j+1}. Space and time partial derivatives of $K(M)$ are approximated by

$$\frac{\partial K(M)}{\partial x} \simeq \theta \frac{K_{i+1}^{j+1} - K_i^{j+1}}{\Delta x_i} + (1 - \theta) \frac{K_{i+1}^j - K_i^j}{\Delta x_i} \quad \dots \dots \dots \dots \dots \quad (8)$$

$$\frac{\partial K(M)}{\partial t} \simeq \frac{K_i^{j+1} + K_{i+1}^{j+1} - K_i^j - K_{i+1}^j}{2\Delta t^j} \quad \dots \dots \dots \dots \dots \quad (9)$$

The second writer (7) found that for slowly varying transients in large rivers, $\theta = 0.55$ minimizes the loss of accuracy associated with greater values while

avoiding the possibility of a weak or pseudo-instability, which may occur when $\theta = 0.50$ is used.

Numerical Solution of Advection Equations.—The implicit weighted four-point finite difference scheme used in the routing model DNRT (6,7) is also applied in DSTEMP. Substituting Eqs. 7, 8, and 9 into the advection equation (Eq. 6) yields

$$\frac{1}{2\Delta t^j}[(AT)_i^{j+1} + (AT)_{i+1}^{j+1} - (AT)_i^j - (AT)_{i+1}^j] + \frac{\theta}{\Delta x_i}[(QT)_{i+1}^{j+1} - (QT)_i^{j+1}]$$

$$+ \frac{(1-\theta)}{\Delta x_i}[(QT)_{i+1}^j - (QT)_i^j] - \frac{\theta}{2}\left\{\frac{C_1}{\rho c_p}(b_i^{j+1} + b_{i+1}^{j+1}) + \frac{C_3}{\rho c_p}(P_i^{j+1} + P_{i+1}^{j+1})\right.$$

$$+ [(Q_i^+ T_i)_i^{j+1} + (Q_i^+ T_i)_{i+1}^{j+1}] + [(q_g^+ PT_g)_i^{j+1} + (q_g^+ PT_g)_{i+1}^{j+1}] + [(q_r bT_r)_i^{j+1}$$

$$\left. + (q_r bT_r)_{i+1}^{j+1}]\right\} - \frac{(1-\theta)}{2}\left\{\frac{C_1}{\rho c_p}(b_i^j + b_{i+1}^j) + \frac{C_3}{\rho c_p}(P_i^j + P_{i+1}^j) + [(Q_i^+ T_i)_i^j\right.$$

$$\left. + (Q_i^+ T_i)_{i+1}^j] + [(q_g^+ PT_g)_i^j + (q_g^+ PT_g)_{i+1}^j] + [(q_r bT_r)_i^j + (q_r bT_r)_{i+1}^j]\right\}$$

$$- \frac{\theta}{2}\left\{\frac{C_2}{\rho c_p}[(bT)_i^{j+1} + (bT)_{i+1}^{j+1}] + \frac{C_4}{\rho c_p}[(PT)_i^{j+1} + (PT)_{i+1}^{j+1}] + [(Q_i^- T)_i^{j+1}\right.$$

$$\left. + (Q_i^- T)_{i+1}^{j+1}] + [(q_g^- PT)_i^{j+1} + (q_g^- PT)_{i+1}^{j+1}] - [(q_e bT)_i^{j+1} + (q_e bT)_{i+1}^{j+1}]\right\}$$

$$- \frac{(1-\theta)}{2}\left\{\frac{C_2}{\rho c_p}[(bT)_i^j + (bT)_{i+1}^j] + \frac{C_4}{\rho c_p}[(PT)_i^j + (PT)_{i+1}^j] + [(Q_i^- T)_i^j\right.$$

$$\left. + (Q_i^- T)_{i+1}^j] + [(q_g^- PT)_i^j + (q_g^- PT)_{i+1}^j] - [(q_e bT)_i^j + (q_e bT)_{i+1}^j]\right\} = 0 \quad (10)$$

In DSTEMP, Q_i^+, Q_i^-, and T_i are assumed invariant over each Δx_i subreach. In the general nomenclature of Eqs. 7, 8, and 9, this invariance can be expressed, for Δx_i, as

$$K_i^j = K_{i+1}^j \quad\dots\dots\dots\dots\dots\dots\dots\dots\dots\dots \quad (11)$$

and $\quad K_i^{j+1} = K_{i+1}^{j+1} \quad\dots\dots\dots\dots\dots\dots\dots\dots\dots\dots \quad (12)$

Also q_g^+, q_g^-, T_g, q_r, T_r, and q_e are assumed invariant over a subreach, Δx_i, and a time interval, Δt^j. In the case of invariance of T_r over Δt^j, for example, it is assumed that the value of wet-bulb temperature is the average value over the time interval, Δt^j. Invariance of q_r over Δt^j implies that q_r is the depth of precipitation cumulated over the time interval Δt^j. In the general nomenclature of Eqs. 7, 8, and 9, the invariance over Δx_i and Δt^j can be expressed as

$$K_i^j = K_{i+1}^j = K_i^{j+1} = K_{i+1}^{j+1} \quad\dots\dots\dots\dots\dots\dots\dots \quad (13)$$

Eq. 10 is rearranged into the following general form after substitution of Eqs. 11, 12, and 13, applied to the appropriate variables:

$$A_i T_i^{j+1} + B_i T_{i+1}^{j+1} = C_i T_i^j + D_i T_{i+1}^j + E_i \quad\dots\dots\dots\dots\dots \quad (14)$$

in which A_i, B_i, C_i, D_i, and E_i are coefficients that are independent of T. Eq. 14 was then solved for T_{i+1}^{j+1} as

$$T_{i+1}^{j+1} = \frac{C_i T_i^j + D_i T_{i+1}^j + E_i - A_i T_i^{j+1}}{B_i} \quad \ldots \ldots \ldots \ldots \ldots \ldots \ldots \ldots (15)$$

Program Capabilities.—The DSTEMP can be applied to the prediction of mean daily stream temperatures and to the prediction of the diurnal variation of stream temperatures. Time and space steps in DNRT and DSTEMP are specified by the user. Successive time steps need not be of equal length. Also, subreaches of different lengths can be specified. The program is structured in a flexible manner, so that individual components of heat transfer across the stream boundaries can be omitted through user options. A choice between three alternative techniques of calculating incident and solar radiation flux at the stream surface has been provided previously. These techniques range from the direct use of observed data to the calculation of solar radiation flux from meteorologic and astronomical data. The calculation approach provides for coefficient estimation to account for local factors affecting solar radiation. A separate subroutine is used to calculate each component of net heat transfer at the stream surface and the streambed. Therefore, a technique currently used to estimate one of the heat transfer components may be readily replaced by another technique without extensive changes to the main program.

A feature of the meteorologic data requirements is the use of meteorologic data sets. A meteorologic data set comprises a complete set of data for all the meteorologic variables required in DSTEMP. Several meteorologic data sets may be used for modeling a stream system. Each data set is applied to a different group of subreaches for which the observed meteorologic data in the data set are considered representative. Provision has been made to treat surface and subsurface lateral inflows separately. A different temperature may be specified for each. In this way, unmodeled tributaries, overland flow, interflow, return flows, etc., can be separated from baseflow originating in the ground-water body. Both surface and subsurface lateral inflows can be negative; in this case they are outflows from the river, and the temperature associated with them is the stream temperature.

Any number of first-order tributaries to the main stream can be handled by DNRT and DSTEMP, providing dimension statements are adjusted to the appropriate size. Thermal loads located as point sources are handled by a simple heat balance procedure. Stream temperatures immediately upstream and downstream of the location at which the point load enters the stream are calculated and output. Two types of output tables are used: A table of stream temperatures, advective heat sources, and hydraulic data for each computational point at each time point; and a table of components of heat exchange at stream surface and bed for each subreach at each time interval. A comprehensive users manual is contained in Ref. 4.

APPLICATION TO BRAZOS-LITTLE RIVER SYSTEM

A search was made for a river system on which to demonstrate the Dynamic Stream Temperature Model (DSTEMP) and its linkage to the Implicit Dynamic Routing Program (DNRT). The following criteria were selected for the river

system: (1) A river-tributary system is preferred to a single river; (2) streamflow and stream temperature data should be available at the upstream boundaries of the main river and tributary and at the downstream boundary of the main river; (3) streamflow at the upstream boundaries of the river system should contribute the major portion of the streamflow at the downstream boundary and therefore lateral inflow should be small; (4) no reservoirs between upstream and downstream boundaries; and (5) no major sources of thermal pollution of streamflow for which records do not exist. The third criterion was established because streamflow-stream temperature modeling in a river system with large lateral inflow becomes mainly a problem of estimating lateral inflow rates and lateral inflow temperatures. In order that the predictions from DSTEMP should not be dominated by lateral inflow temperature estimates, a river system with small lateral inflow was sought such that hydrograph-thermogram routing and
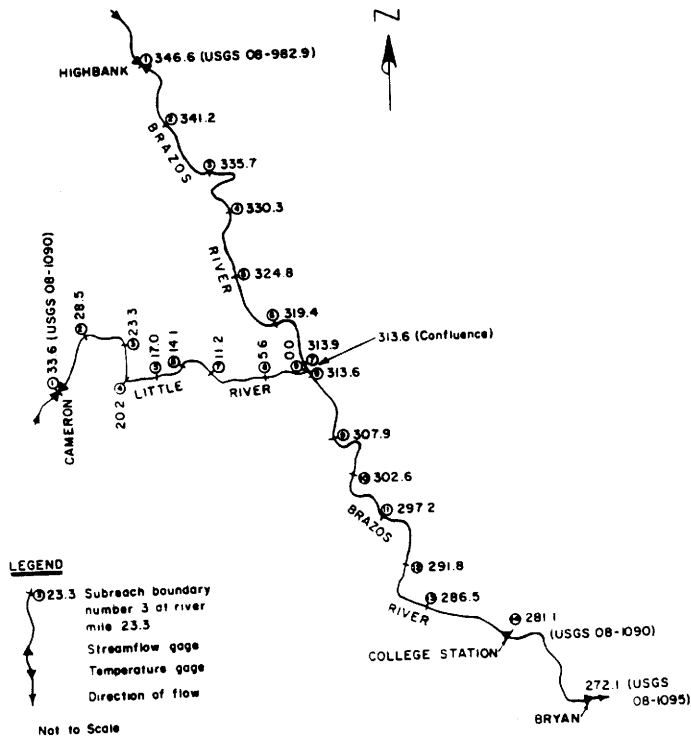
FIG. 3.—Schematic of Brazos-Little River System (1 mile = 1.61 km)

meteorologic considerations were the most important aspects of the stream temperature simulation. After an extensive search, the Brazos-Little Rivers in Texas were found to reasonably satisfy the criteria previously listed.

Brazos-Little River System.—The section of the Brazos-Little River System modeled in this study is bounded by USGS streamflow gages at Highbank, Cameron, and College Station (Fig. 3). Stream temperature records are available at the Highbank and Cameron gages, but not at College Station. Stream temperature records from the Bryan gage, 9.0 miles (14 km) downstream, were used for comparison with stream temperatures predicted by the DSTEMP model at College Stations. On the basis of channel characteristics, the 65.5-mile (105-km) section of the Brazos River was divided into 13 subreaches, and the 33.6-mile (54-km) section of the Little River was divided into eight subreaches.

Data Sources.—Several floods during the 1973 water year were selected for

possible simulation. Streamflow and stream temperature data were obtained from the USGS Surface Water Records and Water Quality Records. Topographic quadrangle maps, and rating curves and cross sections for the gaging stations were furnished by the USGS, Austin, Tex. Meteorologic data were taken from Local Climatic Data published by NOAA. Additional unpublished meteorologic data for College Station were supplied on microfilm from the National Climatic Center, Asheville, N.C. Solar radiation data observed at College Station were made available by the Texas State Climatologist.

Streamflow Modeling.—Cross sections at the gaging stations are triangular-shaped with varying side slopes. Cross sections at points between gaging stations were assumed similar in shape and size. Manning roughness coefficients were computed from available cross sections, rating curves, and the channel bottom slope of 1.1 ft/mile (0.21 m/km), determined from topographic maps. Final calibration of DNRT for unsteady flow conditions consisted of a trial-and-error determination of the lateral inflow, which comprised approx 10% of the total flow, by minimizing the root-mean-square deviation between the observed and simulated flows at College Station. Output from the calibrated DNRT model was written onto computer disk storage files and then read as input by the DSTEMP model.

DSTEMP Problem Setup.—All components of surface heat transfer available in the current version of DSTEMP were used, but streambed heat transfer components were considered negligible. Solar radiation was calculated using the third technique. A 12-hr computational time increment was used. Surface and subsurface components of lateral inflow were lumped together, and no point sources of thermal effluents were represented. Initial temperatures along the river system were estimated by linear interpolation between the upstream and downstream boundaries, while maintaining a heat balance at the confluence of the two rivers. Comparison of observed and predicted stream temperatures was possible at only one location, the downstream boundary. Standard values of the various meteorologic coefficients listed in Ref. 4 were used in this application. Three meteorologic data groups were defined: (1) Brazos River, subreaches 1-7, using precipitation and dry bulb air temperatures observed at Highbank and other meteorologic data from Waco; (2) Little River, subreaches 1-8, using precipitation and dry bulb air temperatures observed at Cameron and other meteorologic data from Waco; and (3) Brazos River, subreaches 9-13, using meteorologic data observed at College Station. Solar radiation data from College Station were used in all three meteorologic data groups. All meteorologic data were input for a meteorologic time interval of 24 hr, except solar radiation data which were input for the 12-hr computational time intervals.

DSTEMP Calibration.—The strategy for calibration of DSTEMP was as follows:

1. Adjust coefficients affecting surface heat-transfer components. Atmospheric radiation and back radiation components are by coefficients for which values are well established and, therefore, these components were not adjusted. The solar radiation component was adjusted by varying S within reasonable limits. Evaporation and conduction components were adjusted by varying N.

2. Adjust estimate of lateral inflow thermogram.

During the early stage of model calibration, the first technique for calculating

solar radiation was used. However, a comparison of solar radiation predicted by this technique, with values observed at College Station, indicated that low values were generally overestimated and that high values were generally un-
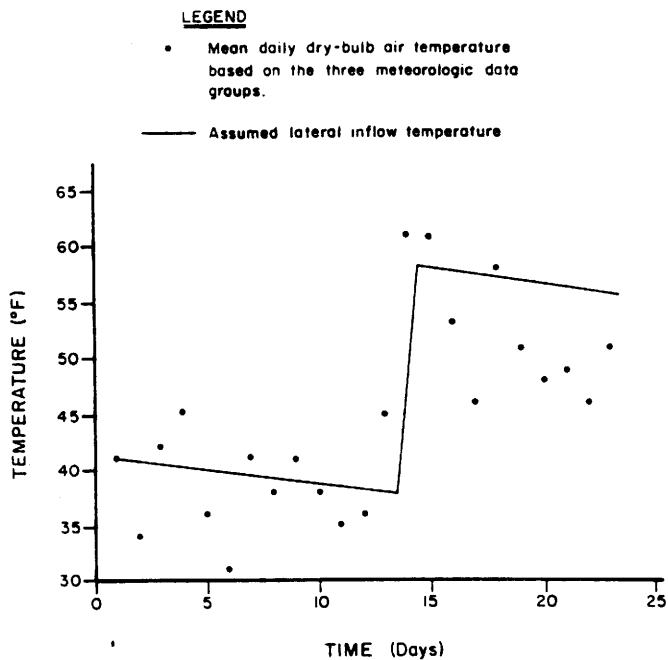
FIG. 4.—Assumed Lateral Inflow Thermogram (1° F = 1.8° C + 32)
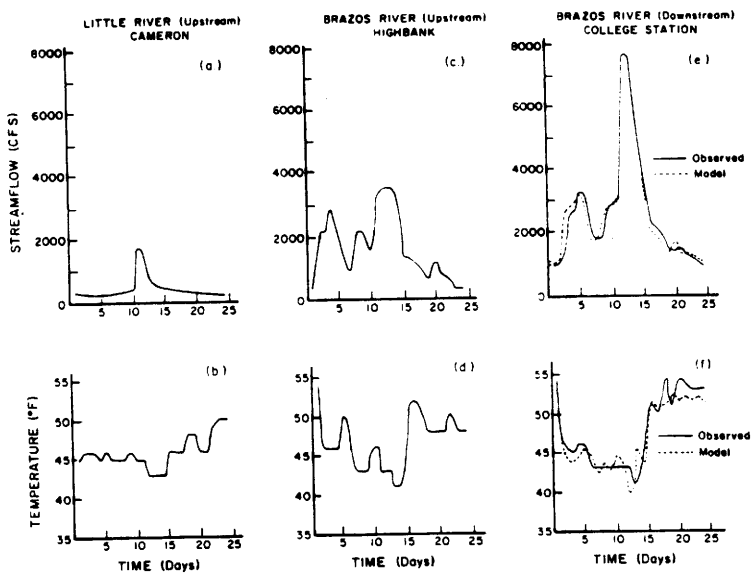
FIG. 5.—Hydrographs and Thermograms at Upstream and Downstream Boundaries of Brazos-Little River System, Including Model Predictions, December 5–28, 1972 (1 cfs = 0.028 m³/s; 1° F = 1.8° C + 32)

derestimated. Therefore, it was decided to use the observed solar radiation data directly.

The USGS at Austin, Tex., estimated shading (S) on the Brazos River to be 5% and on the Little River to be 25%. These values were reduced to 0%

BRAZOS RIVER (HIGHBANK-BRYAN) AND LITTLE RIVER (CAMERON-CONFLUENCE) TEXAS - 24:00 HRS DEC 5 - 24:00 HRS DEC 28, 1972

STREAM TEMPERATURES, ADVECTIVE HEAT SOURCES, AND HYDRAULIC DATA

TIME PT NO 15   DAY 347 HOUR 24.00

| COMP PT NO	RIVER DISTANCE MILES	X-SECTN AREA FT2	TOP WIDTH FT	WETTED PERIM FT	SUB-RCH LENGTH FT	LATINF. TRIBINF FT2S-1	GRDWTR INFLOW FT2S-1	POINT LOAD CFS	STREAM -FLOW CFS	NET GP -FLOW NO	LATIN GNEAF TEMP DF	PT TEMP DF	LD TEMP DF	HEATEX /FT2 /DT BTU	CALCULATED D/STM DF	U/STM DF	OBSER -VED DF
MAIN																	
1	346.60	511.68	169.28	169.28	28512.00	0.0006	.00000	0.00	2090.00	1	39.25	0.00	0.00	63.	43.00		
2	341.20	531.19	172.47	172.47	29040.00	0.0006	.00000	0.00	2057.87	1	39.25	0.00	0.00	62.	43.06		
3	335.70	401.73	164.25	164.25	28512.00	0.0006	.00000	0.00	1990.39	1	39.25	0.00	0.00	61.	43.10		
4	330.30	517.36	170.21	170.21	29040.00	0.0006	.00000	0.00	1907.09	1	39.25	0.00	0.00	60.	43.13		
5	324.80	423.84	154.06	154.06	28512.00	0.0006	.00000	0.00	1823.18	1	39.25	0.00	0.00	59.	43.18		
6	319.40	527.01	171.92	171.92	29040.00	0.0006	.00000	0.00	1730.96	1	39.25	0.00	0.00	58.	43.26		
7	313.90	326.27	135.17	135.17	3168.00	0.1257	.00000	0.00	1672.19	3	44.28	0.00	0.00	30.	43.35		
TRIB1																	
1	33.60	96.93	48.23	48.23	26928.00	0.0006	.00000	0.00	297.00	2	39.25	0.00	0.00	-8.	45.00		
2	28.50	112.67	52.00	52.00	27456.00	0.0006	.00000	0.00	312.52	2	39.25	0.00	0.00	-6.	44.72		
3	23.30	100.05	49.00	49.00	16368.00	0.0006	.C0000	0.00	328.30	2	39.25	0.00	0.00	-5.	44.64		
4	20.20	78.95	43.53	43.53	16896.00	0.0006	.00000	0.00	337.91	2	39.25	0.00	0.00	-4.	44.61		
5	17.00	117.25	53.05	53.05	15312.00	0.0006	.00000	0.00	347.63	2	39.25	0.00	0.00	-2.	44.60		
6	14.10	58.27	37.40	37.40	15312.00	0.0006	.00000	0.00	357.20	2	39.25	0.00	0.00	-1.	44.57		
7	11.20	147.05	59.57	59.57	29568.00	0.0006	.0C000	0.00	365.42	2	39.25	0.00	0.00	2.	44.53		
8	5.60	88.24	46.02	46.02	29568.00	0.0006	.00000	0.00	386.12	2	39.25	0.00	0.00	5.	44.47		
9	0.00	198.47	69.02	69.02					396.52						44.28		
MAIN																	
0	313.30	573.44	194.54	194.54	28512.00	0.0006	.00000	0.00	2059.19	3	39.25	0.00	0.00	36.	43.61		
9	307.90	550.93	190.69	190.69	27984.00	0.0006	.00000	0.00	1995.24	3	39.25	0.00	0.00	37.	43.60		
10	302.60	544.53	189.58	189.58	28512.00	0.0006	.00000	0.00	1937.67	3	39.25	0.C0	0.00	38.	43.68		
11	297.20	535.10	187.93	187.93	28512.00	0.0006	.00000	0.00	1884.01	3	39.25	0.C0	0.00	39.	43.69		
12	291.80	523.02	185.79	185.79	27984.00	0.0006	.00000	0.00	1839.91	3	39.25	0.00	0.00	41.	43.63		
13	286.50	509.10	183.30	183.30	28512.00	0.0006	.0C000	0.00	1802.46	3	39.25	0.00	0.00	42.	43.55		
14	281.10	525.04	186.15	186.15					1771.48						43.45		43.00

FIG. 7.—Stream Temperatures, Advective Heat Sources, and Hydraulic Data Computed by DNRT-DSTEMP at 24:00 hr on Day 7

and 15% respectively, for winter conditions. Heat transfer by evaporation and conduction across the stream surface and directly proportional to the mass transfer coefficient, N. A value of $N = 0.00005$ in. Hg^{-1} $(0.2 \ N \ m^{-2})$ was found to yield reasonable values of evaporation and conduction. Data for the temperature of lateral inflow were not available. It would be difficult to measure representative values of lateral inflow temperature. Perhaps the best approach for establishing this boundary condition would be to link DNRT-DSTEMP to a two-dimensional hydrology-water temperature model. For the study period, the lateral inflow thermogram was found to be highly dependent on air temperature. A lateral inflow thermogram (Fig. 4) based on the variation in air temperature was obtained by a trial-and-error procedure involving several model runs.

Results.—Figs. 5(a) and 5(b) show the upstream streamflow boundary conditions for the dynamic routing model, DNRT, for the period of December 5–28, 1972. A comparison of the observed and predicted hydrographs at the downstream boundary is represented by Fig. 5(e). This figure indicates that very good agreement was achieved between model responses and observed flows. The following factors should be considered when evaluating the adequacy of the stream-temperature simulation results:

1. Thermographs used by the USGS are rated by the manufacturer as accurate to within $2.0°$ F $(1.1°$ C) (12).

2. Observed stream temperatures used in this study were based on USGS instantaneous values which are selected randomly within 24-hr intervals on the continuous thermogram trace. In contrast, model predictions were for time points spaced 12 hr apart. Therefore, a comparison between a predicted and an observed mean temperature may be a comparison between temperatures with up to 24 hr difference in occurrence.

3. DSTEMP predicts stream temperatures that are average for the stream cross section, whereas observed stream temperatures are measured at single locations in the cross section.

4. The observed thermogram in this study was located 9.0 miles (14 km) downstream of the point at which stream temperatures were predicted, resulting in a phase difference of about 4 hr.

Upstream boundary conditions for stream temperature are shown in Figs. 5(b) and 5(d). Observed and predicted thermogram at the downstream boundary are represented by Fig. 5(f). A trough in the predicted thermogram coincides with the peak of the hydrograph [Fig. 4(e)] at day 12 but misses the trough in the observed thermogram by one day. Predicted temperatures after day 16 are generally low compared with observed temperatures. Overall agreement is quite good, with a correlation coefficient, R^2, equal to 0.84 and an average absolute error of $1.39°$ F $(0.77°$ C). Figs. 6 and 7 contain examples of DNRT-DSTEMP output for day 7 of the simulation.

A summary of the surface heat exchange components for reach 13 on the Brazos River is contained in Table 1. The heat exchange values for each component in row 1 were obtained by summing, over the 23-day flood, the absolute values of calculated heat exchange for each time interval. On this basis, the most important component of the total surface heat exchange during the December

BRAZOS RIVER (HIGHBANK-BRYAN) AND LITTLE RIVER (CAMERON-CONFLUENCE) TEXAS   -   24:00 HRS DEC 5 - 24:00 HRS DEC 20, 1972

COMPONENTS OF HEAT EXCHANGE AT STREAM SURFACE AND BED

TIME INTERVAL NO 15   SIZE DT= 12. HRS   (DAY 347 HOUR 24.00 TO DAY 348 HOUR 12.00)

ALL UNITS ARE BTU/FT-2 PER DT IN HRS

REACH NO	SOLAR RADIATION INCIDT	REFLEC	ABSORP	VEGTN RADTN INCIDT REFLEC		ATMOS RADTN INCIDT REFLEC		BACK RACTN	EVAP LHVAP	CCND	SACH LHFUS	SURF RENEW	BECAB SCLAD	EACH BECRD	BED COAD	BED EXCHGE	SLRF EXCHGE	BED EXCHGE
TRIB1																		
1	254.	-20.	234.	0.	0.	1063.	-32.	-1296.	-44.	-20.	0.	0.	0.	0.	0.	0.	-95.	0.
2	254.	-20.	234.	0.	0.	1063.	-32.	-1291.	-43.	-19.	0.	0.	0.	0.	0.	0.	-88.	0.
3	254.	-20.	234.	0.	0.	1063.	-32.	-1288.	-42.	-18.	0.	0.	0.	0.	0.	0.	-83.	0.
4	254.	-20.	234.	0.	0.	1063.	-32.	-1287.	-41.	-18.	0.	0.	0.	0.	0.	0.	-80.	0.
5	254.	-20.	234.	0.	0.	1063.	-32.	-1285.	-41.	-17.	0.	0.	0.	0.	0.	0.	-78.	0.
6	254.	-20.	234.	0.	0.	1063.	-32.	-1284.	-41.	-17.	0.	0.	0.	0.	0.	0.	-77.	0.
7	254.	-20.	234.	0.	0.	1063.	-32.	-1283.	-40.	-17.	0.	0.	0.	0.	0.	0.	-75.	0.
8	254.	-20.	234.	0.	0.	1063.	-32.	-1282.	-40.	-16.	0.	0.	0.	0.	0.	0.	-74.	0.
MAIN																		
1	299.	-24.	275.	0.	0.	1055.	-32.	-1279.	-39.	-19.	0.	0.	0.	0.	0.	0.	-39.	0.
2	299.	-24.	275.	0.	0.	1055.	-32.	-1278.	-38.	-18.	0.	0.	0.	0.	0.	0.	-36.	0.
3	299.	-24.	275.	0.	0.	1055.	-32.	-1276.	-38.	-18.	0.	0.	0.	0.	0.	0.	-34.	0.
4	299.	-24.	275.	0.	0.	1055.	-32.	-1276.	-38.	-17.	0.	0.	0.	0.	0.	0.	-33.	0.
5	299.	-24.	275.	0.	0.	1055.	-32.	-1275.	-38.	-17.	0.	0.	0.	0.	0.	0.	-32.	0.
6	299.	-24.	275.	0.	0.	1055.	-32.	-1275.	-38.	-17.	0.	0.	0.	0.	0.	0.	-32.	0.
7	299.	-24.	275.	0.	0.	1033.	-31.	-1276.	-58.	-30.	0.	0.	0.	0.	0.	0.	-86.	0.
8	299.	-24.	275.	0.	0.	1033.	-31.	-1277.	-58.	-30.	0.	0.	0.	0.	0.	0.	-88.	0.
9	299.	-24.	275.	0.	0.	1033.	-31.	-1277.	-58.	-30.	0.	0.	0.	0.	0.	0.	-88.	0.
10	299.	-24.	275.	0.	0.	1033.	-31.	-1277.	-58.	-30.	0.	0.	0.	0.	0.	0.	-88.	0.
11	299.	-24.	275.	0.	0.	1033.	-31.	-1277.	-58.	-30.	0.	0.	0.	0.	0.	0.	-88.	0.
12	299.	-24.	275.	0.	0.	1033.	-31.	-1277.	-58.	-30.	0.	0.	0.	0.	0.	0.	-88.	0.
13	299.	-24.	275.	0.	0.	1033.	-31.	-1276.	-58.	-30.	0.	0.	0.	0.	0.	0.	-87.	0.

FIG. 6.—Components of Nonadvective Heat Exchange Computed by DNRT-DSTEMP for Time Interval 12:00–24:00 hr on Day 7

flood is solar radiation (row 2). The relative importance of the net surface heat exchange and the lateral inflow heat exchange is also of interest. The absolute values of these two quantities were summed over the 23-day flood

TABLE 1.—Surface Heat Exchange Components for Brazos River (Reach 13) from Simulation of December 5–28, 1972 Flood

Component (1)	Solar radiation adsorped (2)	Net long-wave radiation (back radiation-atmospheric radiation) (3)	Evapora-tion (4)	Conduc-tion (5)	Total surface heat exchange (6)
Heat exchange, in British thermal units per square foot (kilojoules per square meter)	13,872 (1,221)	9,012 (793)	2,496 (220)	3,792 (334)	29,172 (2,568)
Percentage of total surface heat exchange contributed by each component	47	31	9	13	100

TABLE 2.—Net Surface Heat Exchange and Lateral Inflow Heat Exchange for Brazos River (Reach 13) from Simulation of December 5–28, 1972 Flood

Component (1)	Net surface heat exchange (2)	Lateral inflow heat exchange (3)	Overall heat exchange (4)
Heat exchange, in British thermal units per square foot (kilojoules per square meter)	6,420 (565)	2,292 (202)	8,712 (767)
Percentage of overall heat exchange contributed by the net surface and lateral inflow heat exchanges	74	26	100

and are shown in Table 2. These results indicate that 74% of the overall heat exchange is accounted for by the net surface heat exchange.

CONCLUSIONS

Coupled dynamic streamflow and stream temperature models (DNRT-DSTEMP) have been developed and applied. It is considered that DNRT-DSTEMP

3. Bowen, I. S., "The Ratio of Heat Losses by Conduction and by Evaporation From Any Water Surface," *Physical Review*, Vol. 27, July, 1926, pp. 779–787.
4. Bowles, D. S., Comer, L. E., and Grenny, W. J., "Dynamic Stream Temperature Model for Unsteady Flows," Utah Water Research Laboratory, College of Engineering, Utah State University, Logan, Utah, 1975.
5. Comer, L. E., Bowles, D. S., and Grenny, W. J., "Field Investigations and Mathematical Model for Heat Transfer Processes in the Bed of a Small Stream," Utah Water Research Laboratory, College of Engineering, Utah State University, Logan, Utah, 1975.
6. Fread, D. L., "Technique for Implicit Dynamic Routing in Rivers with Tributaries," *Water Resources Research*, Vol. 9, No. 4, Aug., 1973, pp. 918–926.
7. Fread, D. L., "Implicit Dynamic Routing of Floods and Surges in the Lower Mississippi," presented at the April 8–12, 1973, American Geophysical Union Spring National Meeting, held at Washington, D.C.
8. McKee, J. E., and Wolf, H. W., *Water Quality Criteria*, 2nd ed., California State Water Quality Control Board, Sacramento, Calif., 1963.
9. Novotny, V., and Krenkel, P. A., "Heat Transfer in Flowing Streams," *Report No. 7*, Department of Environmental and Water Resources Engineering, Vanderbilt University School of Engineering, Nashville, Tenn., Sept., 1971.
10. Pluhowski, E. J., "Urbanization and Its Effect on the Temperature of the Streams on Long Island, New York," *United States Geological Survey Professional Paper 627-D*, United States Geological Survey, Washington, D.C., 1970.
11. Raphael, J. M., "Prediction of Temperature in Rivers and Reservoirs," *Journal of the Power Division*, ASCE, Vol. 88, No. PO2, Proc. Paper 3200, July, 1962, pp. 157–181.
12. Rawson, J., "Reconnaissance of Water Temperature of Selected Streams in Southeastern Texas," *Report 105*, Texas Water Development Board, Austin, Tex., 1970, p. 2.
13. Wunderlich, W. O., "Heat and Mass Transfer Between a Water Surface and the Atmosphere," *Report No. 14*, Water Resources Research Laboratory, Tennessee Valley Authority, Norris, Tenn., Apr., 1972.

12929 DYNAMIC STREAMFLOW-TEMPERATURE MODELS

ABSTRACT: Current interest in stream temperature prediction stems largely from concern for the possible deleterious environmental consequences of thermally polluted surface waters. Stream temperature is an important determinant of the solubility of dissolved gases, biological reaction kinetics, the distribution of fish and lower forms of aquatic life, and the efficiency of water treatment for domestic and industrial use. This paper describes the Dynamic Stream Temperature Model (DSTEMP). The model is suitable for prediction of stream temperatures over a diurnal cycle and over extended periods of time. DSTEMP may be used for unsteady flow conditions by linkage with a dynamic streamflow routing model (DNRT). Alternatively steady flow conditions may be specified. Data requirements are realistic in terms of data types usually collected by the National Weather Service, NOAA, and the United States Geological Survey. In addition to describing the model an application of DNRT-DSTEMP to the Brazos-Little Rivers, Texas, is included to illustrate that the models provide a practical tool for streamflow-stream temperature forecasting.

offers a very flexible tool for the dynamic simulation of streamflow-stream temperature. The current version of DNRT-DSTEMP is suitable for application in temperature simulation on small streams or large river systems. This versatility is enhanced by the capability of substituting different methods of calculating heat-transfer components, or suppressing components that are unimportant on certain streams. Thus, a stand-alone version of DSTEMP was used in a study of the significance of streambed heat exchange on a small mountain stream (5). Also, the simulation of stream temperature regimes in large river systems is facilitated by the use of meteorologic data groups and by coupling with the DNRT unsteady flow model. Dynamic aspects of the flow and temperature variations, such as those simulated by DNRT-DSTEMP, are essential to obtain predictions of critical, but transient, stream temperature conditions that may endanger aquatic environments.

Table 2 shows that surface heat exchange is more important than lateral inflow heat exchange in the heat balance of reach 13 of the Brazos River during the December 1972 flood. This result demonstrates that the third criterion for selecting a river system was satisfied by the Brazos-Little system. However, the need for considering lateral inflow in this study, and the need for good estimates of lateral inflow temperatures, is demonstrated by the significant role that lateral inflow heat exchange plays in the overall heat exchange, even though lateral inflows accounted for only 10% of the total flow. At present, the estimation of lateral inflow thermograms is mainly the result of intuitive guesses and trial-and-error matching of observed and predicted thermograms after the nonadvective heat transfer process is calibrated. An independent verification of the model is difficult because of the diverse characteristics of lateral inflow thermograms associated with different floods. Therefore, it would be necessary to perform a new trial-and-error estimation of the lateral inflow thermogram for each flood simulated. Thermograms for lateral inflows could be generated by linkage with a two-dimensional hydrology-water temperature model.

APPENDIX.—REFERENCES

1. Amein, M., and Fang, C. S., "Implicit Flood Routing in Natural Channels," *Journal of the Hydraulic Division*, ASCE, Vol. 96, No. HY12, Proc. Paper 7773, Dec., 1970, pp. 2481–2500.
2. Anderson, E. R., "Energy-Budget Studies, Water Loss Investigations: Lake Hefner Studies," *Society of Construction Superintendents Professional Paper 269*, Society of Construction Superintendents, New York, N.Y., 1954.